Polymer 50 (2009) 441–446

Contents lists available at ScienceDirect

Polymer

journal homepage: www.elsevier.com/locate/polymer

Carbon dioxide/propylene oxide coupling reaction catalyzed by chromium salen complexes

Yongsheng Niu [a,b], Wanxi Zhang [a], Hongchun Li [a,b], Xuesi Chen [b,*], Jingru Sun [b], Xiuli Zhuang [b], Xiabin Jing [b]

[a] Key Laboratory of Automobile Materials of Ministry of Education, College of Materials Science and Engineering, Jilin University, Changchun 130022, China
[b] State Key Laboratory of Polymer Physics and Chemistry, Changchun Institute of Applied Chemistry, Chinese Academy of Sciences, Graduate School of Chinese Academy of Sciences, Changchun 130022, China

ARTICLE INFO

Article history:
Received 4 August 2008
Received in revised form
4 November 2008
Accepted 13 November 2008
Available online 18 November 2008

Keywords:
Carbon dioxide
Propylene oxide
Alternating copolymerization

ABSTRACT

A series of chromium/Schiff base complexes *N*,*N*′-bis(salicylidene)-1,2-phenylenediamino chromium^{III} X were prepared and employed for the alternating copolymerization of carbon dioxide with racemic propylene oxide in the presence of (4-dimethylamino)pyridine. The effect of the complex structure and reaction conditions on the catalytic activity, the poly(propylene carbonate)/cyclic carbonate (PPC/PC) selectivity, and the polymer head-to-tail linkages was examined. The experiments indicated that *N*,*N*′-bis(3,5-di-*tert*-butylsalicylidene)-1,2-phenylenediamino chromium^{III} (NO_3) exhibited the highest PPC/PC selectivity as well as polymer head-to-tail linkages and *N*,*N*′-bis(3,5-dichlorosalicylidene)-1,2-phenylenediimino chromium^{III} (NO_3) possessed the highest catalytic activity among these chromium/Schiff base complexes. The structure of the produced copolymer was characterized by the IR, ^{1}H NMR, and ^{13}C NMR measurements. Almost 100% carbonate content of the resulting polycarbonate were obtained with the help of these effective catalyst systems under facile conditions.

1. Introduction

Over the past decade a variety of transition metal Schiff base catalysts or catalyst precursors for the copolymerization of propylene oxide (PO) and carbon dioxide (CO_2) have been reported [1,2], because the resultant polycarbonate is one of the most important synthetic biodegradable polymers investigated for a wide range of pharmaceutical and biomedical applications [3,4]. After zinc catalysts [4–7] and chromium porphyrinates [8,9], chromium salen complexes exhibited extremely super excellence catalytic capability for the CO_2/cyclohexene oxide (CHO) coupling reaction [1]. A variety of efficient catalysts or catalyst precursors for the copolymerization of CHO and CO_2 and a few accounts of very active catalysts for the copolymerization of CO_2 and PO have been reported recently [3,10–12]. In such cases, the main products are cyclic carbonate and/or no reaction occurs between CO_2 and PO. Therefore, the alternating copolymerization of CO_2 and PO is one of the most challenging subjects in the CO_2 fixation field.

Some researches are focused on how to promote the efficiency of polymerization and activity of catalysts [13–15]. The catalyst structure should play an important role in overall catalyst performance. Our objective is to delineate the effect of altering the electronic environments around the metal center by changing the phenoxide substituents of the salen ligand and observe the effect of these changes on the catalytic activity for poly(propylene carbonate) formation.

In the present work, a series of chromium/Schiff base complexes *N*,*N*′-bis(salicylidene)-1,2-phenylenediamino chromium^{III} X (Fig. 1) were prepared and employed for the alternating copolymerization of CO_2 with racemic propylene oxide (*rac*-PO) in the presence of (4-dimethylamino)pyridine (DMAP), and its reaction formation of equation is listed in Scheme 1. The influence of the salen ligand structure on the catalytic activity, the poly(propylene carbonate)/cyclic carbonate(PPC/PC) selectivity, and the polymer head-to-tail linkages was explored. Meanwhile, the influence of copolymerization variables like catalyst component, operating pressure and temperature on the catalytic activity, PPC/PC selectivity, and the molecular weight was discussed in detail. The copolymers were characterized by NMR and FT-IR spectroscopies as well as by means of DSC, GPC, and TGA.

2. Experimental section

2.1. Materials

All manipulations involving air- and/or water-sensitive compounds were carried out using standard Schlenk techniques

* Corresponding author. Tel./fax: +86 431 85262112.
E-mail address: xschen@ciac.jl.cn (X. Chen).

0032-3861/$ – see front matter
doi:10.1016/j.polymer.2008.11.008

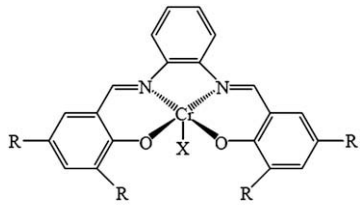

Fig. 1. Structure of complexes **1a** and **1b**–**3b**.

under dry argon. *rac*-PO was refluxed over CaH_2, and fractionally distilled under an argon atmosphere prior to use. CO_2 (99.9995%) was purchased from Changchun Institute of Special Gases and used as received. Diethyl ether was distilled from sodium benzophenone. Methylene chloride, hexane, and chloroform were distilled from CaH_2 under argon. *N*,*N*′-Bis(salicylidene)-1,2-phenylenediimine, *N*,*N*′-bis(3,5-di-*tert*-butylsalicylidene)-1,2-phenylenediimine, *N*,*N*′-bis(3,5-dichlorosalicylidene)-1,2-phenylenediimine were prepared according to the reported method [16,17].

2.2. Measurements

Nuclear magnetic resonance (NMR) spectra were recorded on a Bruker AV 300M instrument in $CDCl_3$ at room temperature. Chemical shifts were given in parts per million using tetramethylsilane. Gel permeation chromatographic (GPC) measurements were carried out with a Waters instrument (515 HPLC pump) equipped with a Wyatt interferometric refractometer. GPC columns were eluted with THF at 25 °C at 1 mL min^{-1}. The molecular weights were calibrated against polystyrene standards. IR spectra were recorded on a Perkin–Elmer 2000 FTIR spectrometer. All the mass spectra were performed by electrospray ionization mass spectrometry (ESIMS). The experiment was performed on a Micromass Q-Tof (Micromass, Wythenshawe, UK) mass spectrometer equipped with an orthogonal electrospray source (Z-spray) operated in positive and negative ion mode. ESIMS spectra in positive ion mode were referenced against the sample of $(m/z)^+ = 574.3182$ (Capillary = 2000 V, Sample cone = 20 V), and those in negative ion mode were referenced against the sample of $(m/z)^- = 193.0898$ (Capillary = 2000 V, Sample cone = 30 V).

2.3. Synthesis of salen chromium complexes **1a** and **1b**–**3b**

2.3.1. Synthesis of complex **1a**

The ligand *N*,*N*′-bis(3,5-dichlorosalicylidene)-1,2-phenylenediimine (1.82 g, 4.0 mmol) and $CrCl_2$ (0.59 g, 4.8 mmol) were dissolved in 50 mL THF and stirred under argon at ambient temperature for 24 h. Then the reaction mixture was exposed to air and stirred for an additional 24 h. After the reaction mixture was poured into diethyl ether (150 mL), the organic layer was washed with aqueous saturated NH_4Cl (3 × 200 mL) and brine (3 × 200 mL) followed by drying with anhydrous Na_2SO_4. After filtration to remove solid impurities and drying agent, solvent was removed in vacuo, yielding a dark brown powder [18]. Yield: 92%. Elemental analysis calcd (%) for $C_{20}H_{10}Cl_5CrN_2O_2$: C, 44.52; H, 1.87; Cr, 9.64; N, 5.19; found: C, 44.44; H, 1.78; Cr, 9.61; N, 5.06. Selected IR data (KBr, cm^{-1}): 1628s, *v*C=N; 1520w, *v*C=C; 1375w, *v*C–N; 1290w, *v*C–O; 580w, *v*Cr–O; 357w, *v*Cr–N. HRMS (*m*/*z*, $M^+ + H$): 501.8714, calcd for $[C_{20}H_{10}Cl_4N_2O_2Cr]^+$ ($[\mathbf{1a} - Cl]$)$^+$: 501.8902.

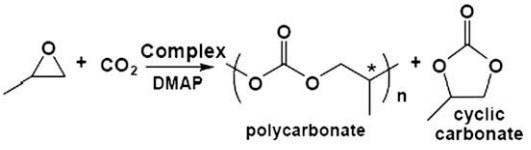

Scheme 1. Reaction of CO_2/*rac*-PO to form linear poly(propylene carbonate) and cyclic carbonates.

2.3.2. Synthesis of complex **1b**

To a stirred mixture of $AgNO_3$ (0.713 g, 4.2 mol) in CH_3CN (80 mL), a solution of complex **1a** (1.08 g, 2.0 mmol) and CH_3CN (80 mL) was added dropwise for 30 min. Immediate precipitation of AgCl was observed, and the reaction mixture was further stirred for 24 h. After filtration to remove solid impurities and drying agent, solvent was removed in vacuo, yielding a dark brown powder. Yield: 93%. Elemental analysis calcd (%) for $C_{20}H_{10}Cl_4CrN_3O_5$: C, 42.43; H, 1.78; Cr, 9.18; N, 7.42; found: C, 42.34; H, 1.67; Cr, 9.22; N, 7.34. Selected IR data (KBr, cm^{-1}): 1632s, *v*C=N; 1541w, *v*C=C; 1373w, *v*C–N; 1293w, *v*C–O; 557w, *v*Cr–O; 367w, *v*Cr–N. HRMS (*m*/*z*, $M^+ + H$): 501.8714, calcd for $[C_{20}H_{10}Cl_4N_2O_2Cr]^+$($[\mathbf{1b} - NO_3]$)$^+$: 501.8902.

2.3.3. Synthesis of complex **2b**

It was synthesized following a similar procedure of complex **1b**. Yield: 90%. Elemental analysis calcd (%) for $C_{20}H_{14}CrN_3O_5$: C, 56.08; H, 3.29; Cr, 12.14; N, 9.81; found: C, 56.01; H, 3.17; Cr, 12.07; N, 9.77. Selected IR data (KBr, cm^{-1}): 1638s, *v*C=N; 1541w, *v*C=C; 1371w, *v*C–N; 1296w, *v*C–O; 541w, *v*Cr–O; 373w, *v*Cr–N. HRMS (*m*/*z*, $M^+ + H$): 366.0371, calcd for $[C_{20}H_{14}N_2O_2Cr]^+$ ($[\mathbf{2b} - NO_3]$)$^+$: 366.0460.

2.3.4. Synthesis of complex **3b**

It was synthesized following a similar procedure of complex **1b**. Yield: 94%. Elemental analysis calcd (%) for $C_{36}H_{46}CrN_3O_5$: C, 66.24; H, 7.10; Cr, 7.97; N, 6.44; found: C, 66.18; H, 7.05; Cr, 7.84; N, 6.32. Selected IR data (KBr, cm^{-1}): 1630s, *v*C=N; 1522w, *v*C=C; 1375w, *v*C–N; 1291w, *v*C–O; 579w, *v*Cr–O; 368w, *v*Cr–N. HRMS (*m*/*z*, $M^+ + H$): 590.2678, calcd for $[C_{36}H_{46}N_2O_2Cr]^+$ ($[\mathbf{3b} - NO_3]$)$^+$: 590.2964.

2.4. Representative copolymerization procedure

A 100 mL Parr autoclave was heated to 120 °C under vacuum for 6 h, then cooled under vacuum to room temperature. A mixture of complex **1b** and DMAP was dissolved in *rac*-PO under nitrogen atmosphere. The mixture solution was stirred for about 10 min and then injected into the autoclave equipped with a magnetic stirrer under a CO_2 atmosphere. The autoclave was heated to a desired temperature in an oil bath and under the appropriate pressure of CO_2. The mixture was stirred for the allotted reaction time, then cooled to room temperature and vented in a fume hood. A small aliquot of the resultant polymerization mixture was removed from the reactor for ^1H NMR analysis. The remaining polymerization mixture was then dissolved in chloroform, quenched with 5% HCl solution in methanol, and precipitated from methanol. The polymer was collected and dried in vacuo to constant weight, and the polymer yield was determined.

3. Results and discussion

3.1. Alternating copolymerization of CO_2 and rac-PO

In the metal-catalyzed epoxide/CO_2 copolymerization, both the axial group X of the complex and the substituent groups on the phenoxide of the salen ligand often exert a significant influence on

the catalytic activity, the polycarbonate/cyclic carbonate selectivity, and the polymer head-to-tail linkages [6,19–23]. Our objective is to delineate further the effect of altering the electronic and steric environments around the chromium center by changing the axial group X of the complex and the substituents on the phenoxide of the salen ligand and observing the effect of these changes on the copolymerization reaction. The alternating copolymerization of CO_2 with *rac*-PO was examined by the **1a** and **1b**–**3b**/DMAP catalyst systems under 1.5 MPa CO_2 at 40 °C, as shown in Table 1. First, the effect of the axial group X on the copolymerization of the CO_2 with *rac*-PO was investigated. The changing in the axial X group of the complex from Cl to NO_3 results in an increase in the PPC/PC selectivity and the head-to-tail linkages of the copolycarbonate (Runs 1 and 2 in Table 1). These results might be mainly ascribed to the electronic effect of the axial X group in terms of greater advantages for the ring opening of *rac*-PO to form Cr–OR as the catalytic living center, which in the initial stage was the rate determining step in the copolymerization reaction [6]. The initial rate of carbonate chain grew which ultimately leaded to produce linear polycarbonates by successive insertion of CO_2/*rac*-PO towards the Cr–O bond as compared with the formation of cyclic carbonates by a back-biting reaction from the propagating alkoxide [1a]. At the same time, the axial group X of complex also plays a role in determining the order of the catalytic activity of these catalysts considering that the catalytic activity of complex **2b** is obviously higher than that of complex **1a**. Then, the effect of the substituent R on the phenoxide of the ligand on the catalytic activity of the complex was discussed. As it can be seen from Runs 2–4 in Table 1, the ligand series show a marked substituent effect, the *rac*-PO conversion and the PPC/PC selectivity, as well as the polymer head-to-tail linkages are sensitive to the subtle changes in the ligand structure. It can be seen that the effect of the substituent R on the phenolate of the ligand in complexes **1b**–**3b** on their catalytic activity is obvious. With the R being an electron-withdrawing chlorine group, the **1b**/DMAP catalyst system displays a high catalytic activity ($TOF_{PC} = 16\ h^{-1}$, $TOF_{PPC} = 162\ h^{-1}$; Run 2 in Table 1). Under the same conditions, when the R group is replaced by a hydrogen atom, the **2b**/DMAP catalyst system exhibits a lower catalytic activity ($TOF_{PC} = 14\ h^{-1}$, $TOF_{PPC} = 148\ h^{-1}$; Run 3 in Table 1); with the R being *tert*-butyl, the **3b**/DMAP catalyst system presents the lowest catalytic activity ($TOF_{PC} = 11\ h^{-1}$, $TOF_{PPC} = 136\ h^{-1}$; Run 4 in Table 1). The catalytic activity of these complexes for the alternating copolymerization of CO_2 with *rac*-PO increases in the order **1b** > **2b** > **3b** (Runs 2–4 in Table 1) under same conditions. These results might be mainly ascribed to the electronic effect of the substituent R on the phenolate of the ligand. While the PPC/PC selectivity as well as polymer head-to-tail linkages increases in the opposition order: **3b** > **2b** > **1b** (Runs 2–4 in Table 1). The bulky substituent R on the phenolate of the ligand influences the ring-opening position of the *rac*-PO incorporated next to the growing polymer chain and thus significantly influences the PPC/PC selectivity and polymer head-to-tail linkages. Both the axial group X of the complex and the substituents on the ligand do not have a clear effect on the resulting copolymer molecular weights.

To optimize the reactivity of this catalyst system further, the influence of catalyst and cocatalyst mole ratio, reaction temperature, and CO_2 pressure on the copolymerization was investigated. Complex **1b** was used to study the effect of the reaction conditions on polymer formation, and some representative results are summarized in Tables 2 and 3.

As a cocatalyst the Lewis bases played a very important role on the *rac*-PO/CO_2 copolymerization. Different cocatalysts were selected in the experiments such as DMAP, *N*-methylimidazole (*N*-MeIm), and tetra-*n*-butyl ammonium bromide (Bu_4NBr), and the results are tabulated in Table 2. For the same amount of 1 equiv Lewis base, the PPC yield from DMAP, Bu_4NBr, and *N*-MeIm was 48.6, 36.3, and 12.6%, respectively, drastically decreasing from DMAP to *N*-MeIm. Moreover, the M_n of PPC from DMAP, Bu_4NBr, and *N*-MeIm was 13700, 9500, and 4100, respectively, nearly 70% decrease from DMAP to *N*-MeIm. Therefore, DMAP was chosen for the following study.

The mole ratio of DMAP to complex **1b** plays an important role in the PPC/PC selectivity and fast production of the polycarbonate. The catalyst system composed of 1 equiv complex **1b** and 2 equiv DMAP was used (Run 1 in Table 3). Only PC was obtained. The PC formation might be based on the presence of a depolymerization reaction that is promoted at higher DMAP concentrations. It is most likely due to a back-biting reaction starting from an alcoholate chain end that is displaced from the Cr^{III} center in a coordination equilibrium with DMAP after epoxide ring opening [24]. The PPC/PC selectivity increases with the decrease of DMAP to complex **1b** mole ratio. The DMAP to complex **1b** mole ratio of 1:1 yields the predominant formation of PPC ($PPC = 182\ h^{-1}$, $PC = 16\ h^{-1}$; Run 2 in Table 3). Further decrease in DMAP to complex **1b** mole ratio is partial to produce PPC, but the catalytic activity decreases. Reactions in the absence of DMAP gave low catalytic activity ($TOF_{PC} = 2\ h^{-1}$, $TOF_{PPC} = 34\ h^{-1}$; Run 4 in Table 3).

On the other hand, the rate of copolymerization varied significantly with pressure. An increase of CO_2 pressure from 0.6 to 1.5 MPa results in a nearly two-fold enhancement in the rate of copolymer formation (Runs 2 and 6 in Table 3). However, the increase of the pressure to 4 MPa results in a significant drop-off in reaction rate. For over 1.5 MPa pressure, the fact that the molecular

Table 1
Effects of the structure of salenCr$^{(III)}$ X on copolymerization of CO_2/*rac*-PO.

Catalyst system[a]		Product					
Run	Complex	*rac*-PO conversion (%)	TOF_{PC}[b] (h^{-1})	TOF_{PPC}[c] (h^{-1})	Polymer		
					Head-to-tail linkages[d] (%)	M_n[e] (10^3)	PDI[e]
1	**1a**	46.8	36	120	80	12.4	1.62
2	**1b**	53.4	16	162	85	13.7	1.45
3	**2b**	48.6	14	148	86	13.2	1.45
4	**3b**	44.1	11	136	88	12.8	1.38

[a] Copolymerizations run in neat *rac*-PO with [*rac*-PO]:[Cr]:[DMAP] = 500:1:1 at 40 °C with 1.5 MPa of CO_2 for 1.5 h. All poly(propylene carbonate)s contain >99% carbonate linkages as determined by ^{1}H NMR spectroscopy.
[b] Turnover frequency of *rac*-PO to cyclic carbonate as determined by ^{1}H NMR spectroscopy.
[c] Turnover frequency of *rac*-PO to poly(propylene carbonate) as determined by ^{1}H NMR spectroscopy.
[d] Determined by ^{13}C NMR spectroscopy.
[e] Determined by GPC.

Table 2
Copolymerization of CO_2/*rac*-PO by complex **1b** and different cocatalyst–catalyst systems.[a]

Run	Cocatalyst	TOF_{PC}[b] (h^{-1})	TOF_{PPC}[c] (h^{-1})	Yield[d] (%)	M_n[e] (10^3)	PDI[e]
1	DMAP	16	162	48.6	13.7	1.45
2	Bu_4NBr	14	121	36.3	9.5	1.31
3	*N*-MeIm	8	42	12.6	4.1	1.24

[a] Copolymerizations run in neat *rac*-PO with [*rac*-PO]:[Cr]:[Cocatalyst] = 500:1:1 at 40 °C with 1.5 MPa of CO_2 for 1.5 h. All poly(propylene carbonate)s contain >99% carbonate linkages as determined by ^{1}H NMR spectroscopy.
[b] Turnover frequency of *rac*-PO to cyclic carbonate as determined by ^{1}H NMR spectroscopy.
[c] Turnover frequency of *rac*-PO to poly(propylene carbonate) as determined by ^{1}H NMR spectroscopy.
[d] Based on isolated PPC yield.
[e] Determined by GPC.

Table 3
Copolymerization of CO_2/*rac*-PO by the **1b**/DMAP catalyst system.

Reaction conditions[a]				Product				
Run	DMAP/ **1b**	Pressure (MPa)	Temperature (°C)	TOF_{PC}[b] (h^{-1})	TOF_{PPC}[c] (h^{-1})	Polymer		
						Yield[d] (%)	M_n[e] (10^3)	PDI[e]
1	2	1.5	40	618	0	–	–	–
2	1	1.5	40	16	182	27.3	25.7	1.45
3	0.5	1.5	40	11	156	23.4	21.4	1.55
4	0	1.5	40	2	34	5.1	5.4	1.18
5	1	4	40	70	81	12.2	13.4	1.51
6	1	0.6	40	11	93	14.0	15.7	1.37
7	1	1.5	20	1	32	4.8	5.2	1.16
8	1	1.5	60	65	201	30.2	17.2	1.55
9	1	1.5	80	432	86	12.9	6.2	1.57

[a] Copolymerization run in neat *rac*-PO (7 mL, 100 mmol) with [*rac*-PO]:[Cr] = 2000:1 for 3 h. All poly(propylene carbonate)s (PPC) contain >99% carbonate linkages as determined by ^{1}H NMR spectroscopy.
[b] Turnover frequency of *rac*-PO to cyclic carbonate as determined by ^{1}H NMR spectroscopy.
[c] Turnover frequency of *rac*-PO to polycarbonate as determined by ^{1}H NMR spectroscopy.
[d] Based on isolated PPC yield.
[e] Determined by GPC.

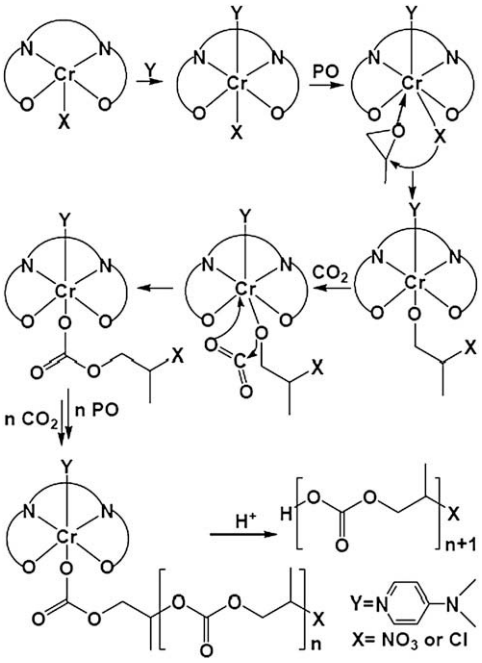

Scheme 2. Proposed mechanism for CO_2/*rac*-PO copolymerization by the complexes/DMAP catalyst systems.

weight of copolymer decreased with increasing pressure might be mainly attributed to that CO_2 solubility increases with the increase of CO_2 pressure and complex **2b** is insoluble in CO_2.

The effect of reaction temperature was a very important factor for the copolymerization. By the **1b**/DMAP catalyst system, the copolymerization of CO_2 and *rac*-PO selectively gave the alternating copolymer at 20 °C in 3 h (PPC = 32 h^{-1}, PC = 1 h^{-1}; Run 7 in Table 3), although the reaction proceeded rather slowly (TOF_{PPC+PC} = 33 h^{-1}). When the temperature was increased to 40 °C, the TOF_{PPC+PC} increased more rapidly to attain 198 h^{-1} in the same reaction time, with slightly lowering the selectivity (PPC = 182 h^{-1}, PC = 16 h^{-1}; Run 2 in Table 3). The decrease of the selectivity for polycarbonate with the temperature increase may be caused by the depolymerization and degradation of the copolymer. Similar results have been observed previously [25]. When the copolymerization was conducted at an elevated temperature, such as 80 °C, a significant amount of cyclic carbonate (PPC = 86 h^{-1}, PC = 432 h^{-1}; Run 9 in Table 3) was generated under otherwise similar conditions. The molecular weight of the obtained copolymer increases with the increasing polymerization temperature until reaching the maximum value at about 40 °C and then begins to decrease.

On the basis of the information presented so far, some proposed mechanism illustrated that the Lewis base coordinated to the metal center in the axial site, *trans* to the propagating metal–polymer chain, thereby labilizing the metal alkoxide bond and facilitating the insertion of CO_2 [1,17]. The *rac*-PO monomer might be first inserted favorably to the Cr–X chemical bond of the Schiff base chromium complexes, followed by the insertion of CO_2 monomer, as shown in Scheme 2. Subsequent alternating enchainment of *rac*-PO and CO_2 affords the alternating polycarbonate. Side reaction of cyclic carbonate could happen through the back-biting degradation of the growing polymer–catalyst complex. A mechanism similar to that proposed by Darensbourg and co-workers using chromium salen and *N*-MeIm in the copolymerization of CO_2 and cyclohexene oxide [1a].

3.2. Structure and properties of the alternating copolymer

The IR spectrum of the PPC copolymer sample (Run 2 in Table 3) is illustrated in Fig. 2. Peaks at 1749 and 1235 cm^{-1} exist in product, which are ascribed to strength vibrations of C=O and C–O, respectively, in oxycarbonyl groups. This indicates the success of the incorporation of CO_2 into the copolymer chain. The ^{1}H NMR spectrum for the corresponding PPC copolymer is shown in Fig. 3. The characteristic peaks in the spectrum are assigned as follows: ^{1}H NMR ($CDCl_3$), δ (ppm) 1.33 (d, 3H; –C<u>H</u>$_3$), 4.18 (m, 2H; –<u>H</u>$_2$C–), 5.0 (d, 1 H; –C<u>H</u>–). By comparison with the ^{1}H NMR spectrum of random PPC copolymer in the literature [26,27], poly(propylene oxide) was observed in the ^{1}H NMR spectrum at 1.16 ppm (d, 3H; –C<u>H</u>$_3$–), 3.58 ppm (2H; –C<u>H</u>$_2$CH–) and 3.45 ppm (1H; –CH$_2$C<u>H</u>–). The poly(propylene oxide) was not observed in the ^{1}H NMR spectrum (Fig. 3). The signals indicate that copolymer is an alternative copolymer. The corresponding ^{13}C NMR spectrum is shown in

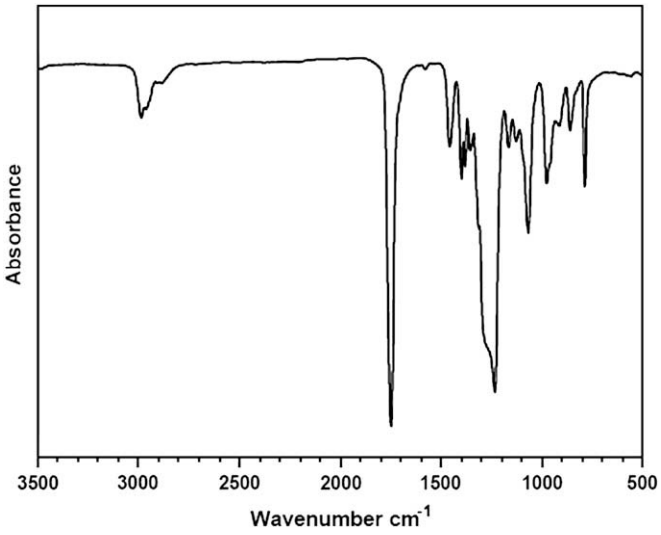

Fig. 2. IR spectrum of poly(propylene carbonate) from the alternating copolymerization of CO_2/*rac*-PO sample procreant by the **1b**/DMAP catalyst system (Run 2 in Table 3).

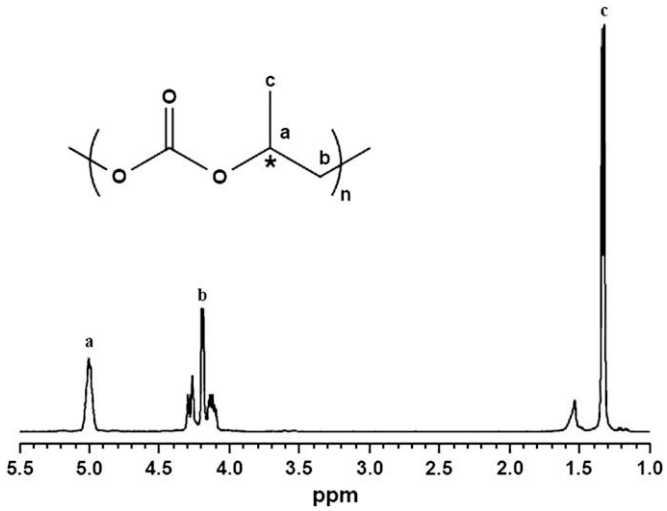

Fig. 3. ^{1}H NMR spectrum of poly(propylene carbonate) from the alternating copolymerization of CO_2/*rac*-PO sample procreant by the **1b**/DMAP catalyst system (Run 2 in Table 3).

Fig. 4. The signals at 16.5, 69.4, 72.7 and 154.6 ppm are assigned to the carbon of $\underline{C}H_3$, $\underline{C}H$, $\underline{C}H_2$ and O$\underline{C}$OO groups, respectively, in the carbonate linkages of the copolymer. It is apparent that there is no poly(propylene oxide) units present in the copolymer product. It can be concluded that the synthesized PPC copolymer exhibits a completely alternating molecular structure.

To further investigate the relationship between the copolymer head-to-tail connectivity and the structure of complex, ^{13}C NMR analyses of the carbonyl region of poly(propylene oxide) obtained from complexes **1a** and **1b**–**3b** were conducted, and the spectra are shown in Fig. 5. Changes in the axial group X of the complex from Cl to NO_3 drastically resulted in copolymer head-to-tail connectivity increasing from 80% to 85% (Fig. 5a and b). The substituent R on the phenolate of the ligand also influenced polymer head-to-tail linkages. If the R was the bulky substituent *tert*-butyl, the **3b**/DMAP catalyst system displayed the highest head-to-tail connectivity (88%, Fig. 5d). When the R group was replaced by an electron-withdrawing chlorine group, polymer head-to-tail connectivity decreased obviously.

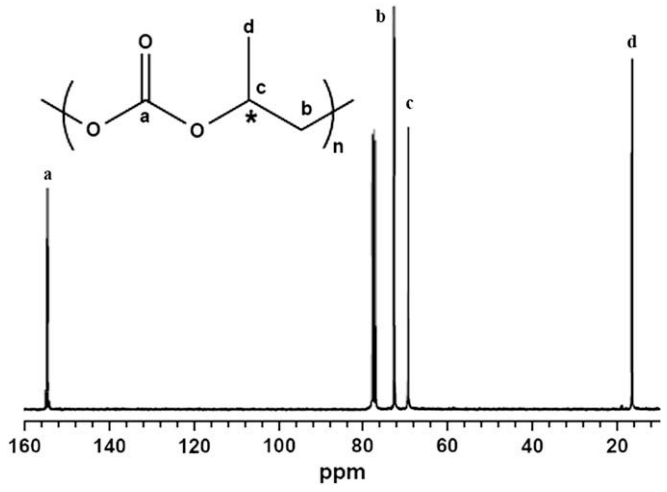

Fig. 4. ^{13}C NMR spectrum of poly(propylene carbonate) from the alternating copolymerization of CO_2/*rac*-PO sample procreant by the **1b**/DMAP catalyst system (Run 2 in Table 3).

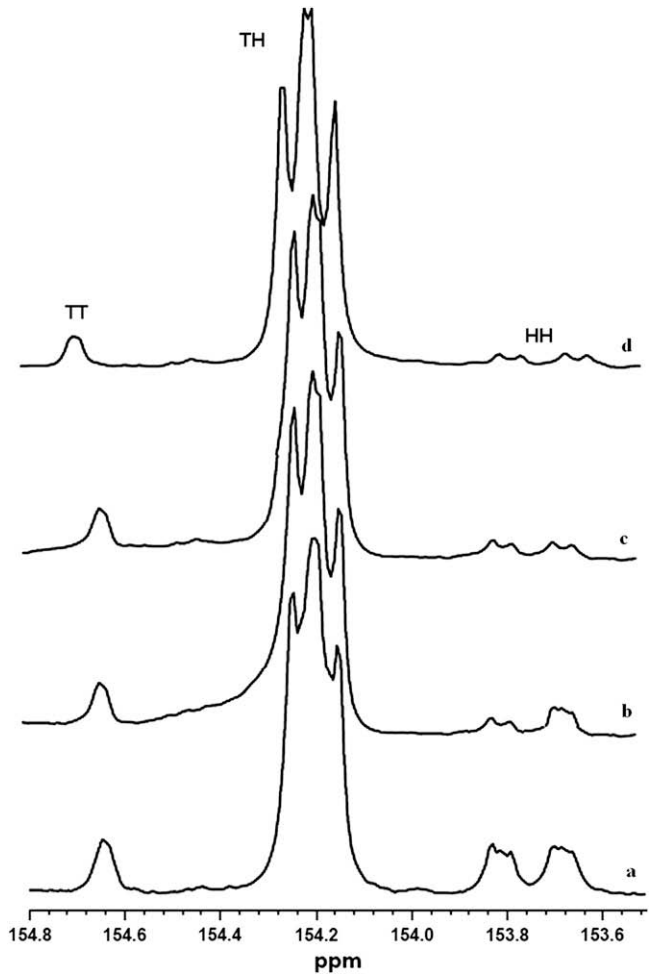

Fig. 5. Carbonyl region of the ^{13}C NMR spectra of poly(propylene carbonate) by the different complexes (a, **1a** (Run 1 in Table 1); b, **1b** (Run 2 in Table 1); c, **2b** (Run 3 in Table 1); and d, **3b** (Run 4 in Table 1)) in the presence of DMAP.

The obtained PPC was amorphous as reported previously in the literature [10,28,29]. Thermal properties of the PPC were determined by DSC and TGA techniques. Glass transition temperature (T_g) was detected to be 32.5 °C in the DSC run under a nitrogen atmosphere, and thermal degradation temperature (T_d) appeared to be 234.6 °C in the TGA run under a nitrogen atmosphere. Both results demonstrate good thermal properties for the produced PPC.

4. Conclusions

In summary, a series of chromium/Schiff base complexes *N*,*N*′-bis(salicylidene)-1,2-benzenediamino chromium^{III} X for the alternating copolymerization of *rac*-PO and CO_2 in the presence of DMAP were investigated. The change in the axial group X of complex from Cl to NO_3 drastically results in an increase in the PPC/PC selectivity and polymer head-to-tail linkages. The influence of the substituent R on the phenolate of the ligand on catalytic activity, PPC/PC selectivity and head-to-tail linkages was studied. The **1b**/DMAP catalyst system exhibits high catalytic activity, while the **3b**/DMAP catalyst systems yield copolymer with high PPC/PC selectivity and head-to-tail linkages. The highly efficient catalysis reaction was observed at mild temperature of 40 °C and a low pressure of 1.5 MPa, with the binary **1b**/DMAP catalyst system (1:1, molar ratio).

Acknowledgement

Gratitude is expressed to the National Natural Science Foundation of China (project No. 20774092, Key Project No. 50733003) and the National Fund for Distinguished Young Scholars (No. 50425309), Chinese Academy of Sciences (KGCX-YW-208).

References

[1] (a) Darensbourg DJ, Yarbrough JC. J Am Chem Soc 2002;124:6335–42;
(b) Darensbourg DJ, Yarbrough JC, Ortiz C, Fang CC. J Am Chem Soc 2003; 125:7586–91;
(c) Darensbourg DJ, Mackiewicz RM, Phelps AL, Billodeaus DR. Acc Chem Res 2004;37:836–44;
(d) Darensbourg DJ, Mackiewicz RM. J Am Chem Soc 2005;127:14026–38;
(e) Darensbourg DJ. Chem Rev 2007;107:2388–410;
(f) Darensbourg DJ, Holtcamp MW. Coord Chem Rev 1996;153:155–74;
(g) Coates GW, Moore DR. Angew Chem Int Ed 2004;43:6618–39.
[2] Eberhardt R, Allmendinger M, Rieger B. Macromol Rapid Commun 2003;24:194–6.
[3] (a) Srivastava R, Srinivas D, Ratnasamy P. Catal Lett 2003;91:133–9;
(b) Srivastava R, Srinivas D, Ratnasamy P. Catal Lett 2003;89:81–5;
(c) Srivastava R, Srinivas D, Ratnasamy P. Stud Surf Sci Catal 2004;154C:2703–10;
(d) Srivastava R, Srinivas D, Ratnasamy P. J Catal 2005;233:1–15;
(e) Srivastava R, Srinivas D, Ratnasamy P. Microporous Mesoporous Mater 2006;90:314–26;
(f) Srivastava R, Srinivas D, Ratnasamy P. Appl Catal A Gen 2005;189:128–34;
(g) Srivastava R, Srinivas D, Ratnasamy P. Tetrahedron Lett 2006;47:4213–7.
[4] (a) Inoue S, Koinuma H, Tsuruta T. J Polym Sci Part B Polym Lett 1969;7:287–92;
(b) Inoue S. Makromol Chem A 1979;13:651–64;
(c) Sugimoto H, Ohshima H, Inoue S. J Polym Sci Part A Polym Chem 2004; 41:3549–55;
(d) Sugimoto H, Inoue S. Pure Appl Chem 2006;78:1823–34.
[5] Soga K, Imai E, Hattori I. Polym J 1981;13:407–10.
[6] (a) Darensbourg DJ, Holtcamp MW. Macromolecules 1995;28:7577–9;
(b) Koning C, Wilderson J, Parton R, Plum B, Steeman P, Darensbourg DJ. Polymer 2001;42:3995–4004.
[7] Cheng M, Lobkovsky EB, Coates GW. J Am Chem Soc 1998;120:11018–9.
[8] Kruper WJ, Dellar DV. J Org Chem 1995;60:725–7.
[9] (a) Mang SA, Cooper AI, Colclough ME, Chauhan N, Holmes AB. Macromolecules 2000;33:303–8;
(b) Stamp LM, Mang SA, Holmes AB, Knights KA, de Miguel YR, McConvey IF. Chem Commun 2001:2502–3.
[10] (a) Super MS, Beckman EJ. Trends Polym Sci 1997;5:236–40;
(b) Super MS, Beckman EJ. Macromol Symp 1998;127:89–108.
[11] Rokicki A, Kuran W. J Macromol Sci Rev Macromol Chem 1981;C21:135–86.
[12] Xiao YL, Wang Z, Ding KL. Macromolecules 2006;39:128–37.
[13] Quan ZL, Wang XH, Zhao XJ, Wang FS. Polymer 2003;44:5605–10.
[14] Chen S, Hua ZJ, Fang Z, Qi GR. Polymer 2004;45:6519–24.
[15] (a) Liu YF, Huang KL, Peng DM, Wu H. Polymer 2006;47:8453–61;
(b) Lu LB, Huang KL. J Polym Sci Part A Polym Chem 2005;43:2468–75.
[16] Schaus SE, Brandes BD, Larrow JF, Tokunaga M, Hansen KB, Gould AE, et al. J Am Chem Soc 2002;124:1307–15.
[17] Darensbourg DJ, Mackiewicz RM, Rodgers JL, Fang CC, Billodeaux DR, Reibenspies JH. Inorg Chem 2004;43:6024–34.
[18] Martinez LE, Leighton JL, Carsten DH, Jacobsen EN. J Am Chem Soc 1995; 117:5897–8.
[19] Darensbourg DJ, Wildeson JR, Yarbrough JC, Reibenspies JH. J Am Chem Soc 2000;122:12487–96.
[20] Lu XB, Wang Y. Angew Chem Int Ed 2004;43:3574–7.
[21] Darensbourg DJ, Zimmer MS, Rainey P, Larkins DL. Inorg Chem 2000;39: 1578–85.
[22] Moore DR, Cheng M, Lobkovsky EB, Coates GW. J Am Chem Soc 2003; 125:11911–24.
[23] Paddock RL, Nguyen ST. Macromolecules 2005;38:6251–3.
[24] Malcolm HC, Diana NL, Zhou ZP. Macromolecules 2002;35:6494–504.
[25] Niu YS, Zhang WX, Pan X, Chen XS, Zhuang XL, Jing XB. J Polym Sci Part A Polym Chem 2007;45:5050–6.
[26] Jung JH, Ree M, Chang T. J Polym Sci Part A Polym Chem 1999;37:3329–36.
[27] (a) Gao LJ, Xiao M, Wang SJ, Du FG, Meng YZ. J Appl Polym Sci 2007;104: 15–20;
(b) Meng YZ, Du LC, Tiong SC, Zhu Q, Hay AS. J Polym Sci Part A Polym Chem 2002;40:3579–91.
[28] Lee YB, Choi JH. J Korean Ind Eng Chem 1996;7:813–22.
[29] Zhu Q, Meng YZ, Tjong SC, Zhao XS, Chen YL. Polym Int 2002;51:1079–85.